39th Joint Propulsion Conference AIAA 2003-4560
Huntsville Alabama, 21-23 July 2003

ANALYTICAL MODEL OF ELECTRON BACKSTREAMING FOR ION THRUSTERS

John D. Williams,[*] Dan M. Goebel,[†] and Paul J. Wilbur[**]

ABSTRACT

Analytical equations historically used to predict the onset of electron backstreaming in ion thrusters tend to underestimate significantly the accel grid voltage required to block electron backflow from the beam plasma because they neglect detailed beamlet focusing and space charge effects inside the grid apertures. We present corrected analytical equations that provide a good estimate of the minimum voltage that must be applied to the accel grid to ensure electron backstreaming is negligible. The equations include terms that account for the effects of voltage penetration induced by screen grids, finite thickness accel grids, and positive space charge associated with ions within accel grid apertures. The backstreaming limit is shown to vary significantly with beamlet current because of ion focusing and associated positive space-charge effects in the accel grid aperture. Calculations of the onset of backstreaming for ion optics designs intended for high specific impulse operation are performed using the analytical equations, and comparisons are made to numerical simulations and experimental results. The analytic and numerical methods give reasonably good agreement with the data, suggesting that the appropriate physics has been included.

INTRODUCTION

To prevent the flow of electrons from the beam plasma through the grids and into the discharge chamber of an ion thruster, it is necessary to apply a sufficiently negative voltage to the accel grid. This eliminates both erroneous ion beam current readings and unwanted beam-supply power losses into the discharge chamber. Enlargement of the accel grid apertures with time due to charge-exchange-induced ion sputtering of the accel grid aperture walls, and the subsequent onset of electron backstreaming at a given accel grid voltage, is one of the primary life limiting mechanism in ion thrusters. In the past, the magnitude of the required anode voltage has been estimated using a simple equation developed by Kaufman[1]. However, Kaufman's equation has been found to underestimate significantly the required accel grid voltage at higher beam current densities and/or higher specific impulses that are presently of interest for deep space propulsion.

An improved model of the accel grid voltage required to prevent backstreaming (called the backstreaming limit) with greater accuracy is desired to enable rapid predictions of this characteristic voltage especially for analysis of grid systems under development where numerical code runs can be too time consuming. If the grid erosion rate is known from short term wear tests or simple sputtering models, an accurate backstreaming model can also facilitate thruster life predictions. It is also noted that accurate predictions of the backstreaming limit will enable operation at lower accel voltages, where charge exchange ion kinetic energies at accel grid impact, and grid wear rates will be lower. Hence grid lifetimes will be greater.

While recently developed numerical models can also be used to predict required voltages with good accuracy, these models are sometimes unavailable or inappropriate for a quick evaluation. As an alternative, we have developed an analytical model for performing rapid predictions of electron backstreaming limits. Our analytical model contains both the effects of the applied potentials and the space charge of the ions as they pass through the accel grid aperture in a simple expression.

APPROACH

Electrons will migrate upstream into the discharge chamber along a path of lowest potential difference from the beam plasma when their upstream kinetic energy exceeds the minimum adverse potential energy decrement they must pass through. For the typical potential profile shown in Fig. 1, the electrons that can backstream would be those with an energy greater than $e(V_{bp} - V_{sp})$. The backstreaming current of Maxwellian electrons at temperature T_e (in eV) that would pass from the beam plasma through the saddle point is given by

$$J_e = \frac{A\, n_e\, e\, v_e}{4}\, e^{-\frac{(V_{bp} - V_{sp})}{T_e}} \quad . \tag{1}$$

where A is the area associated with an ion beamlet at the location where the downstream (beam) plasma becomes neutralized , n_e the electron density in the beam plasma, e the electron charge, m_e the electron mass, and v_e the electron mean thermal velocity given by

$$v_e = \sqrt{\frac{8\, e\, T_e}{\pi\, m_e}} \quad . \tag{2}$$

The current of counter flowing ions is given by:

$$J_b = A\, n_+\, e\, v_+ \ , \tag{3}$$

[*] Senior Member AIAA, Assistant Professor, Colorado State University
[†] Senior Member AIAA, Principal Scientist, Jet Propulsion Laboratory
[**] Senior Member AIAA, Professor, Colorado State University

where n_+ is the ion density across the beamlet area A at the boundary of the beam plasma, and v_+ is the ion velocity given by

$$v_+ = \sqrt{\frac{2\,e\,(V_{dp} - V_{bp})}{m}} \quad , \qquad (4)$$

where m is the ion mass. Combining Eqs. (1) through (4) and assuming equal ion and electron densities in the beam plasma yields the following expression for the local potential minimum:

$$V_{sp}^{*} = V_{bp} + T_e\, \ell n \left[\frac{2\,J_e}{J_b} \sqrt{\pi \left(\frac{m_e}{m} \right) \left(\frac{V_{dp} - V_{bp}}{T_e} \right)} \right]. \qquad (5)$$

This equation gives the "saddle-point" voltage (V_{sp}^{*}) required to limit electron backstreaming that is quantified in terms of a backstreaming-to-beamlet current ratio (e.g., $J_e/J_b = 10^{-3}$). It is noted that the discharge-plasma to beam-plasma potential difference is the net accelerating voltage of the ions. The difference between beam plasma potential and the saddle point potential can be referred to as a retarding potential and is equal to ~8.3 V for a typical beam plasma electron temperature of 1 eV.

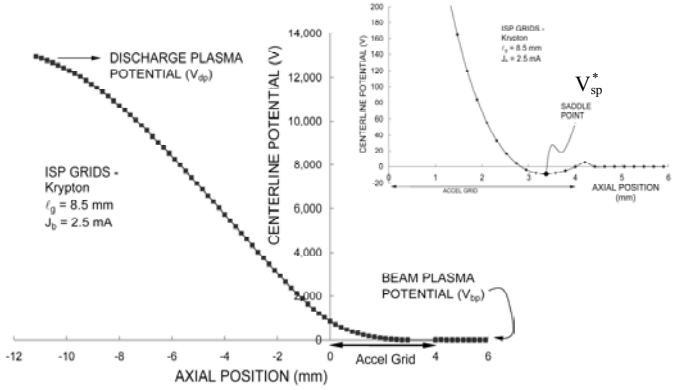

Fig. 1 Typical high Isp grid set potential profiles at the point where backstreaming onset will occur. Inset shows exploded view near the accel grid location.

The voltage that must be applied to the accel grid to induce this saddle-point voltage is determined by the potential environment through which electrons must flow. An idealized 1-D model that can be used to describe this environment is shown in Fig. 2a. It includes an accel grid with a hole having a diameter d_a positioned between two planar surfaces representing the discharge plasma sheath at potential V_{dp} and a downstream beam plasma surface at potential V_{bp}. Neglecting plasma effects, the preferred potential path through which beam plasma electrons will backstream is along the z axis and the point of greatest negative potential along this path is the classic electrostatic saddle point (V_{sp}). For an infinitesimally thin accel grid, the saddle point potential on the centerline at an axial location z_{sp} is given by[2]

$$V_{sp} = \left[\frac{(V_{dp} - V_a)}{2\,\ell_e} + \frac{(V_{bp} - V_a)}{2\,\ell_d} \right] \left\{ |\,z_{sp}\,| - \frac{d_a}{\pi} \left\{ \frac{2\,z_{sp}}{d_a} \tan^{-1}\left(\frac{d_a}{2\,z_{sp}} \right) - 1 \right\} \right\} + \left[\frac{(V_{bp} - V_a)}{2\,\ell_d} - \frac{(V_{dp} - V_a)}{2\,\ell_e} \right] z_{sp} + V_a \ . \qquad (6)$$

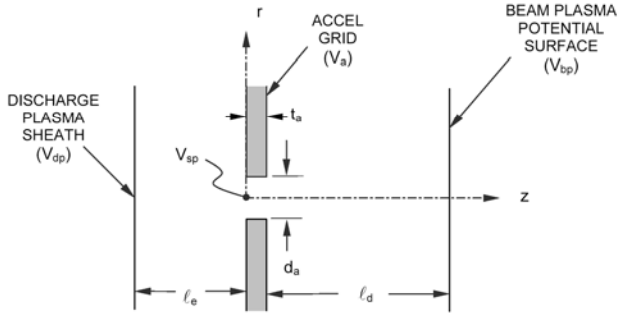

a) Idealized one-dimensional model

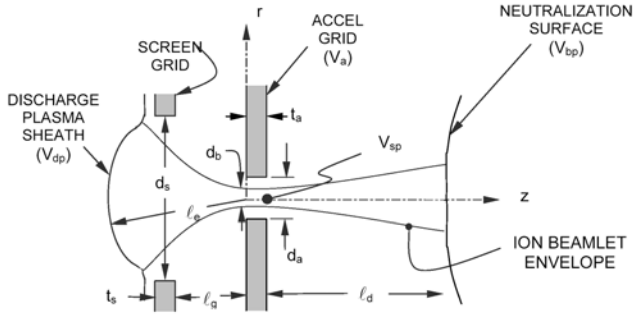

b) Improved model

Fig. 2 Electron backstreaming schematics.

The terms enclosed by the square brackets in Eq. (6) represent the upstream and downstream electric fields at the accel hole and Fig. 1 suggests the upstream electric field is much greater than the downstream value. Although this may not be the case in all applications, numerical analysis of many grid systems of current interest indicates the downstream terms (those that involve division by ℓ_d) can be neglected. It is also noteworthy that Eq. (6) is valid for cases where $d_a < \ell_e$, $d_a < \ell_d$, and $t_a \cong 0$. The first of these conditions is generally met for typical grid systems but the second is not. Kaufman argues, however, on the basis of experimental evidence that the influence of accel grid thickness is described by an accel grid hole aspect-ratio-dependent exponential shielding term.[1] Finally, it is observed that Fig. 1 shows a saddle point that is located near the downstream plane of the accel grid. Analysis of many typical grid systems operating over a wide range of

voltages and beamlet currents suggests that the saddle point is, in fact, generally located near this plane.

When the three simplifications suggested by the observation made above, Eq. (6) becomes

$$V_{sp} = V_a + \frac{d_a (V_{dp} - V_a)}{2\pi \ell_e} \left[1 - \frac{2 t_a}{d_a} \tan^{-1} \left(\frac{d_a}{2 t_a} \right) \right] e^{-\frac{t_a}{d_a}} \quad . \quad (7)$$

The first term on the right-hand side of Eq. (7) represents the negative bias applied to the accel grid to prevent backstreaming and the second term reflects the influence of the positively biased upstream environment (the screen grid potential). Equation (7) needs to be modified, however, so it can be applied to the more realistic beamlet configuration shown in Fig. 2b that accounts for the screen grid aperture and the curvature of the sheath at the discharge chamber plasma boundary. In particular, the length ℓ_e needs to be defined and the effect of ion beamlet space charge needs to be incorporated. The most appropriate value for the effective length ℓ_e is the distance from the accel grid to the plasma sheath, shown in Fig. 2b, which is considered to be

$$\ell_e = \sqrt{(\ell_g + t_s)^2 + \frac{d_s^2}{4}} \quad ,$$

where the dimensions used are defined in the figure. This effective acceleration length has also been used in the Child-Langmuir equation as a good approximation for the distance between two electrodes operated at space-charge-limit conditions.[3]

Since scalar potentials are additive, the effect of the ion space charge in the accel grid aperture can be incorporated by simply adding the potential change induced by the ion space charge. This potential difference (derived in Appendix A) between the beam axis and the accel aperture wall is given by

$$\Delta V = \frac{J_b}{2\pi \varepsilon_o} \left[\frac{m}{2 e (V_{dp} - V_{sp})} \right]^{1/2} \left[\frac{1}{2} - \ell n \left(\frac{d_b}{d_a} \right) \right] . \quad (8)$$

Adding this term directly to the RHS of Eq. (7) gives the saddle-point potential in the accel aperture that accounts for the ion space charge, i.e.,

$$V_{sp}^* = V_a + \Delta V + \frac{d_a (V_{dp} - V_a)}{2\pi \ell_e} \left[1 - \frac{2 t_a}{d_a} \tan^{-1} \left(\frac{d_a}{2 t_a} \right) \right] e^{-\frac{t_a}{d_a}} \quad . \quad (9)$$

In Eqs. (8) and (9), J_b is the beamlet current, d_b/d_a the beamlet-to-accel hole diameter averaged over the length of the accel aperture, and the other symbols have been defined earlier. Because the argument of the logarithm in Eq. (8) is always less than one, values of ΔV will always be positive and this term will, therefore, always cause the saddle-point potential given by Eq. (9) to increase.

Rearranging Eq. (9) gives an expression for the "backstreaming limit", which is the minimum accel grid potential that will reduce the backstreaming current to a specified percent of the beamlet current (e.g., $J_e/J_b = 0.1\%$)

$$V_a = \frac{V_{sp}^* - \Delta V - B V_{dp}}{1 - B} \quad , \quad (10)$$

where

$$B = \frac{d_a}{2\pi \ell_e} \left[1 - \frac{2 t_a}{d_a} \tan^{-1} \left(\frac{d_a}{2 t_a} \right) \right] e^{-\frac{t_a}{d_a}} ,$$

and where V_{sp}^* is given by Eq. (5) and ΔV is given by Eq. (8).

For low specific impulse applications, a simpler equation for the backstreaming limit that is sometimes sufficient is obtained by neglecting space charge and downstream electric field effects and by assuming that the saddle-point potential is at $z_{sp} = 0$ and $V_{bp} = 0$. Noting that the discharge plasma potential is equal to the net accelerating voltage (V_N), Eq. (7) can be rearranged to obtain the following equation for the magnitude of the accel grid voltage required to induce a saddle point potential of zero (i.e., sufficient to stop cold plasma electrons from a beam at zero potential):

$$|V_a| = \frac{V_N}{2\pi \frac{\ell_e}{d_a} e^{\frac{t_a}{d_a}} - 1} . \quad (11)$$

This is the form of the simplified backstreaming limit equation originally given by Kaufman.[1]

MODEL VALIDATION

In order to validate the electron backstreaming model embodied in Eqs. (9) and (10), comparisons were made to both numerical and experimental results obtained from high and low specific impulse grids. The high specific impulse grid set used was developed for the Interstellar Precursor (ISP) Mission, for which extensive electron backstreaming measurements[5] have been published. Critical dimensions and operating conditions associated with the 19-hole ISP gridlet sets that were tested on krypton propellant are given in Table 1.

To calculate the effect of space charge, the beamlet diameter and current density in the accel aperture must be known. We examined the beamlet focusing numerically using the CSU "igx" code.[4] An example showing a typical map of the density of ions in a beamlet that is passing through the exit plane of an accel hole is shown in Fig. 3. Here greater luminosity indicates greater density, and it is apparent from the figure that the density varies in both the radial and azimuthal directions. The radial variations in density are expected from the focusing effect of the grid optics and the aximuthal variations are attributed to perturbations in the local potential near the screen grid due to the neighboring grid apertures. The figure also suggests that the beamlet exhibits a rather well defined outer boundary when its radius is in the range of 70-80% of the accel hole radius.

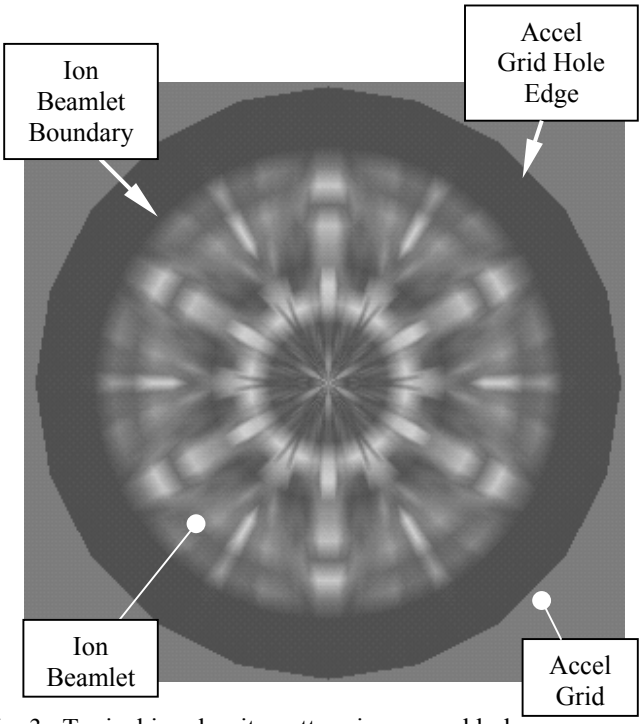

Fig. 3 Typical ion density pattern in an accel hole.

TABLE 1. Design and operating parameters for ISP grids.

Parameter	Symbol	Value	Comment
Accel hole diameter	d_a	4.5 mm	
Accel grid thickness	t_a	4 mm	
Screen hole diameter	d_s	9 mm	
Screen grid thickness	t_s	1.5 mm	
Screen-accel grid gap	ℓ_g		variable: 7 – 10 mm
Center-to-center spacing	ℓ_{cc}	10.4 mm	
Discharge plasma potential	V_{dp}	13.03 kV	
Accel grid voltage	V_a		variable
Beam plasma potential	V_{bp}	0 V	estimated
Beamlet current	J_b		variable

The space charge model represented by Eq. (8) invokes the assumption of a uniform ion density across a beamlet diameter, so it is necessary to resolve data like those in Fig. 3 into a mean density extending to an effective beamlet radius before it can be applied. This was done by looking for the outer radius at which the luminosity drops off. The radius where this occurs was found to be rather well defined as can be seen by the data of Fig. 4. This figure contains a plot of azimuthally averaged values of the Fig. 3 data. It shows a rather well defined beamlet boundary at about 70% of the accel hole diameter, beyond which the profile drops to zero. Profiles determined at other axial positions through accel holes showed similar shapes but would in general have slightly different outer boundary radii. Computations made at several axial locations through the accel aperture were therefore averaged to obtain a mean radius associated with the beamlet over the full thickness of the accel grid.

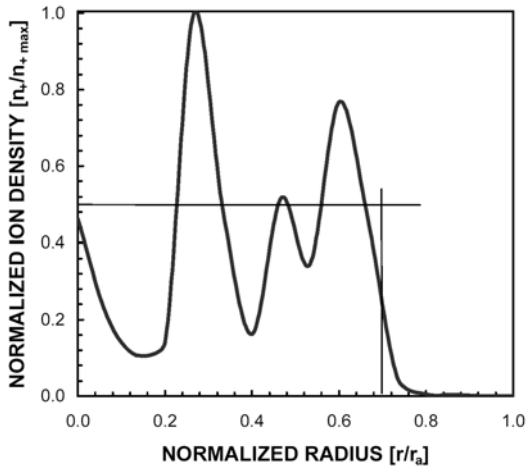

Fig. 4 Typical azimuthally averaged radial ion density profile in an accel hole.

The variation in the ratio of mean beamlet diameter-to-accel hole diameter computed for the ISP grids are shown in Fig. 5 as a function of beamlet current for three different grid spacings. These curves demonstrate an expected behavior that is nevertheless important to note. At low beamlet currents, the grids are operating near the crossover limit and the ion density is finite over a substantial fraction of the accel hole. As the current is increased the diameter of the finite ion density region first decreases until the beamlet is most sharply focused and then rises again up to the point where the perveance limit is reached and the ion density is again finite throughout most of the hole. The accel hole fill factor varies essentially parabolically from the cross over limit to the perveance limit.

While one disadvantage of the analytical model is that the beamlet-to-accel hole diameter ratio must be input into Eq. (8), it should be noted that the logarithm function makes this dependence relatively weak. Adequate precision using the approach described herein may be obtained by defining an approximate function that describes the beamlet focusing level

as a function of beamlet current. From numerical simulation results like those shown in Fig. 5, one could assume that the relative beamlet diameter varies from 0.8 at crossover and perveance conditions and approaches 0.3 at a beamlet current midway between these conditions using a parabola. The simple parabolic fit to these data provides the fill factor diameter ratio needed in Eq. (8).

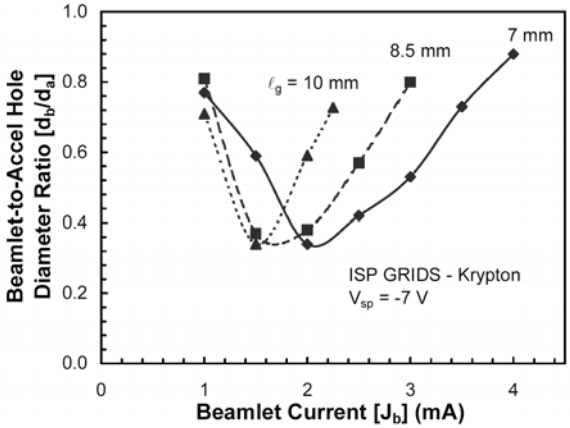

Fig. 5 Beamlet diameter calculations for the ISP grids.

Unfortunately, neither the electron temperature in the beam plasma nor its potential (V_{bp}) were measured during the ISP gridlet tests. However, if we assume reasonable values of T_e=1 eV, and V_{bp}=0 V, the saddle-point potential required to limit the electron backstreaming current to 0.1% of the beam current was computed using Eq. (5). This calculation yields a value of about -8.3 V. When this value, the data of Fig. 5, and the other data of Table 1 are used in Eq. (10), the magnitude of the voltage that must be applied to the accel grid to sustain the specified level of backstreaming can be determined as a function of beamlet current. The results of these calculations are compared in Fig. 6 for three different grid spacings to the corresponding backstreaming limits measured in the laboratory and to our numerical simulations. These data show reasonably good agreement, and in particular are similar in magnitude and trend as beamlet current and grid separation are varied. We note that without the space charge terms in Eq. (8), the analytic results would be a flat line at about 100 V in these plots., This illustrates the significant deficiency in the previous analytic expressions used.

Comparison of the various terms in Eqs. (5), (8), and (10) indicate that the variation in backstreaming limit with beamlet current is due to the space charge of the beamlet passing through the accel hole. Both the magnitude of the charge (determined directly by the beamlet current) and the relative focusing of this charge have an influence and result in maxima that occur between the crossover and perveance beamlet current limits. Furthermore, the voltage rise within the beamlet at the saddle point position due to space charge is typically 10 times greater than the voltage rise at the same point caused by the positive bias of the discharge-plasma/screen-grid boundary.

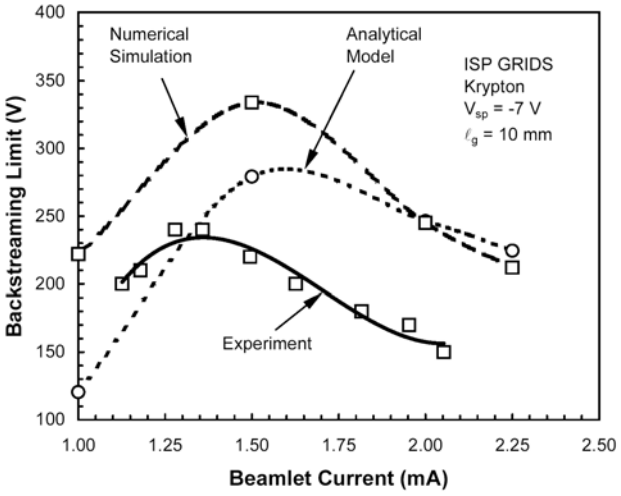

Fig. 6a Backstreaming comparisons at a spacing of 10 mm.

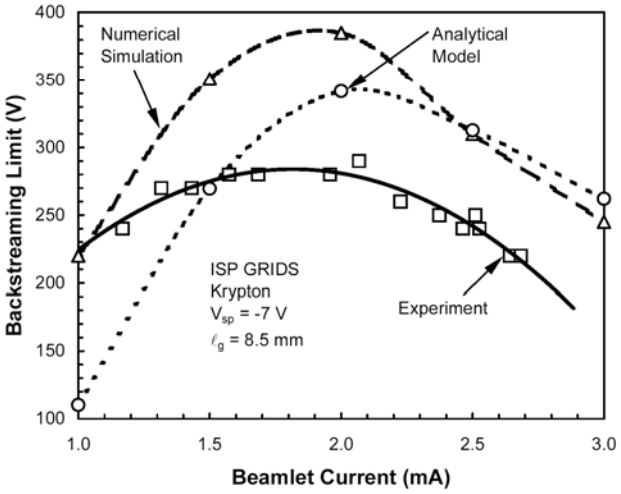

Fig. 6b Backstreaming comparisons at a spacing of 8.5 mm.

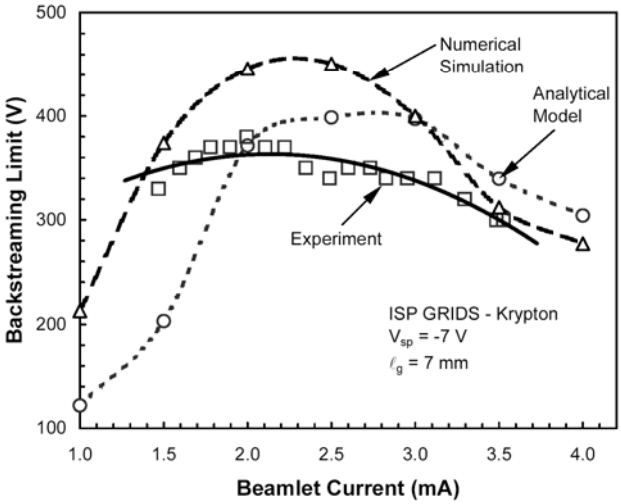

Fig. 6c Backstreaming comparisons at a spacing of 7 mm.

Although our approach was originally developed for high specific impulse grid designs, it is interesting to determine how the analytical model predicts backstreaming behavior in conventional ion optics systems that have higher beam current densities, much smaller ratios of grid separation-to-accel hole diameter, ℓ_g/d_a, and smaller dimensions in general. Quite a bit of information exists on the NSTAR thruster, and this geometry was chosen for additional study. Figure 7 contains data from Soulas and Rawlin on relative beamlet diameter plotted as a function of beamlet current for an NSTAR grid set that had not been operated for a significant amount of time.[6] They observed that the beam diameter increased linearly with beamlet current. These data were used as input to Eq. (10) along with the assumption that the beam plasma potential was 22 V and the saddle point potential at the condition where backstreaming would occur was -13 V. Equation (10) was then solved for the accel voltage and the result is plotted in Fig. 8. The data suggest that the grids will most likely begin to backstream near the thruster centerline where the beamlet current is a maximum and when a voltage magnitude of 98 V is applied to the accel grid. This backstreaming voltage is in reasonable agreement with beginning of life (BOL) measurements made on NSTAR ion thrusters.[7]

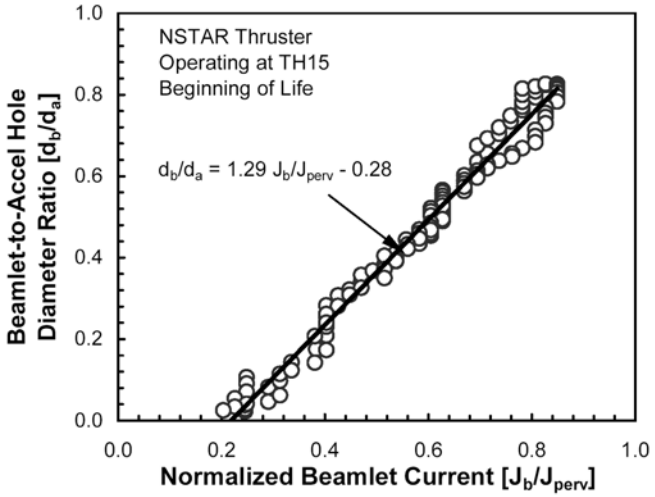

Fig. 7 Variation in NSTAR beamlet diameter as a function of beamlet current (from Soulas and Rawlins, 1999)

Data obtained by Sengupta during an extended life test of the NSTAR ion thruster have showed a gradual increase in the backstreaming voltage as a function of thruster operational time.[7] Optical measurements of the accel grid made during the life test have indicated that the accel hole diameter is slowly enlarging and this erosion process is responsible for the trend observed in the backstreaming measurements.[7,8]

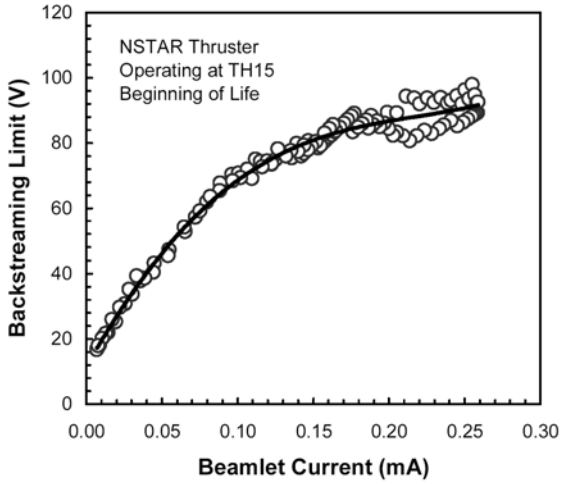

Fig. 8 Analytical prediction of the backstreaming limit for the NSTAR thruster as a function of beamlet current calculated using measured beamlet diameters from Soulas and Rawlin (1999).

To make comparisons to life test data, we exercised the model contained in Eq. (10), and also performed numerical simulations as a function of accel hole diameter. The results of this work are plotted in Fig. 9. It is noted that the numerical simulations are very similar to life test measurements, and they are shown to be higher than the analytical model predictions. The solid square data points shown in Fig. 9 were found using a BOL experimental beamlet diameter from Fig. 7 (d_a = 0.79 mm) and by assuming that this diameter would remain relatively constant as the accel hole diameter was varied. The open square data points in Fig. 9 were calculated by first determining the beamlet diameter using numerical simulations. These values of the beamlet diameter have been found to be larger than experimentally measured ones reported in Ref. (6), and this has the effect of reducing the ΔV calculated from Eq. (8). Despite differences that are observed depending upon the beamlet diameter used, comparisons of the factors contributing to voltage rise at the saddle point indicate that the space charge effect is still dominate for the NSTAR conditions, but not to the extent that it is for the larger ISP grids, probably due to higher beamlet current and sharper focusing effects in the ISP grid set.

Figure 10 compares backstreaming limits measured on gridlets fabricated to study **c**arbon-**b**ased **i**on **o**ptics (CBIO) designs[9] that are being considered by JPL. The CBIO grid geometry is scaled to be ~21% larger than typical NSTAR dimensions except for the accel grid thickness, which is 100% thicker than NSTAR. The data displayed in Fig. 10 corresponds to an accel diameter 27% greater than the nominal CBIO accel diameter to simulate EOL conditions. (See Ref. 10 for more details concerning gridlets tests of the CBIO design.) The backstreaming limit data are plotted as a function of net accelerating voltage with corresponding values

determined numerically using the igx code and using the analytical model. The electron temperature and beam plasma potential were chosen to be 30 V and 1 eV for the data sets displayed in Fig. 10. For the calculations, the ratio of backstreaming electron to beam ion currents was set at 0.1%, but it is noted that the experimental data used 2% as the threshold for determining the onset of backstreaming.[9]

The numerical and analytical results in the figure are seen to exhibit trends similar to that of the experimental results. Further, the numerical and experimental results match at the 2.22 kV voltage condition and all numerical and analytical results are within about 30 V of the measured values. Finally, it is noted that the beam plasma electron temperature and potential were not measured and different assumptions could be made to bring all of the data into closer agreement

Although further study related to beamlet diameter sizes and space charge effects is required, it is believed that the analytical model under predicts the NSTAR and CBIO backstreaming limit due to a breakdown in Eq. (7), which is intended to account for effects of boundary conditions and shielding effects of a thick accel grid. Specifically, it is believed that Eq. (7) becomes less accurate as the ratio between grid separation and accel hole diameter, ℓ_g/d_a, is reduced to values significantly below unity.

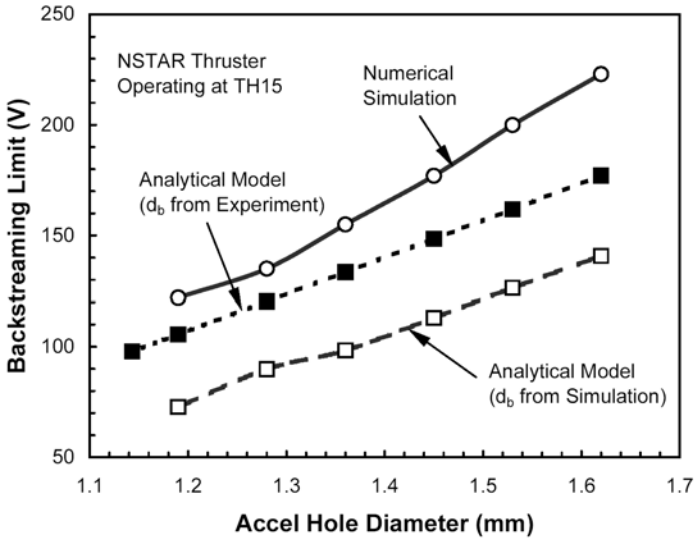

Fig. 9 Comparison of backstreaming limit variation with d_a.

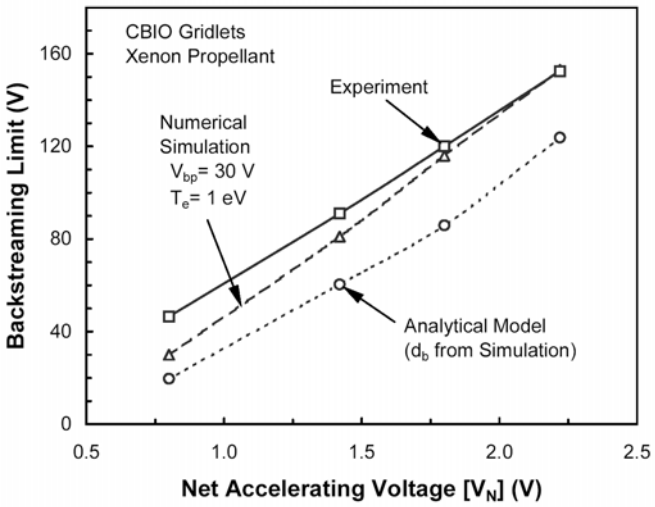

Fig. 10 Comparison of backstreaming limit variation with V_N.

CONCLUSION

We have presented analytical equations that can be used to estimate the minimum voltage magnitude that must be applied to the accel grid to prevent backstreaming. The new equations include elements that account for the effects of applied potentials, thick accel grids, and the positive space charge associated with ion beams that are contained within the accel grid apertures. Calculations of the relative magnitudes of these effects indicate that space charge has a dominate effect, and this result casts doubts on earlier backstreaming models that do not consider space charge. A significant variation in the backstreaming limit is found as a function of beamlet current due to its magnitude and level of ion focusing that occurs near the accel grid location. It is observed that electron backstreaming is most likely to occur at beamlet currents intermediate between perveance and crossover operational limits where the ion focusing effect is strongest. Comparisons between analytical, numerical, and experimental backstreaming voltage calculations and measurements for ion optics designs intended for high specific impulse operation were found to be in reasonable agreement. Similar comparisons made to conventional grid geometries designed for use at lower specific impulse show that the analytical model under predicts the magnitude of the backstreaming voltage. Although further study is needed, we believe this discrepancy is related to the breakdown of assumptions in the element of the analytical model that accounts for applied potentials on the boundaries of the problem. It is suggested that additional experimental and numerical studies of the backstreaming problem be carried out in order to further refine and characterize the analytical model developed to date.

REFERENCES

1. H.R. Kaufman, "Technology of Electron-Bombardment Ion Thrusters", *Advances in Electronics and Electron Physics*, V. 36, pp. 301-303, Academic Press, San Francisco, 1974.
2. K.R. Spangenberg, *Vacuum Tubes,* p. 348, McGraw-Hill, New York, 1948.
3. P.J. Wilbur, J.R. Beattie and J. Hyman, Jr., "An Approach to the Parametric Design of Ion Thrusters," J. Prop. and Power, V. 6, No. 5, Sept.-Oct. 1990, pp. 575-583.
4. Y. Nakayama and P.J. Wilbur, "Numerical Simulation of High Specific Impulse Ion Thruster Optics," Paper IEPC 01-099, International Electric Propulsion Conference, Pasadena, CA, October 2001
5. P.J. Wilbur, J. Miller, C.C. Farnell and V.K. Rawlin, "A Study of High Specific Impulse Ion Thruster Optics," Paper IEPC 01-098, International Electric Propulsion Conference, Pasadena, CA, October 2001.
6. G. Soulas and V.K. Rawlin, " Memorandum: Beamlet Diameter Measurements," NASA Glenn Ion Thruster Team, March 22, 1999.
7. A. Sengupta, J.R. Anderson, and J.R. Brophy, K. Rawlin, and J.S. Sovey, "Performance Characteristics of the Deep Space 1 Flight Spare Ion Thruster Long Duration Test after 21,300 hrs of Operation," AIAA-01-3959, Joint Propulsion Conference, Cleveland, OH, 2002. Also see references cited by this work.
8. J.D. Williams, "Attachment B: A Simple Analytical Model of Accel Grid Lifetime," CSU monthly letter to V.K. Rawlin at NASA Glenn Research Center, October 15, 2002.
9. J.S. Snyder, J.R. Brophy, D.M.Goebel, J.S. Beatty, and M.K. DePano, "Development and Testing of Carbon-Based Ion Optics for 30-cm Ion Thrusters, AIAA-2003- 4716, 39th Joint Propulsion Conference, Huntsville, AL, 2003.
10. D.M. Laufer, J.D. Williams, C.C. Farnell, P.B. Shoemaker, P.J. Wilbur, "Experimental Evaluation of Sub-scale CBIO Ion Optics Systems," AIAA-2003-5165, 39th Joint Propulsion Conference, Huntsville, AL, 2003.

APPENDIX A
The Potential Modification Induced by Ion Space Charge in the Accel Aperture

The effect of the ion space charge associated with an ion beamlet (Fig. 2b) can be accounted for using the following integral form of Gauss's Law:

$$\oint_S \vec{E} \cdot d\vec{A} = \frac{1}{\varepsilon_o} \int_V \rho \, dV \quad . \tag{A1}$$

In Eq. (A1), $\vec{E}$ is the electric field, $d\vec{A}$ is the differential surface area element, ε_o is the permittivity of free space, ρ is the ion charge density within the closed Gaussian surface which has a surface area S and encloses volume V, and dV is a differential volume element. The ion space charge throughout the entire beamlet region shown in Fig. 2b will influence the saddle-point potential, but the charge density effect associated with the right circular cylindrical region defined by the accel-hole will have a dominant effect, especially in the radial direction between the centerline and barrel of the hole. Integration of the left hand side of Eq. (A1) to obtain the radial electric field strength at the cylindrical surface of a Gaussian "pillbox" of radius r in the accel aperture yields

$$\oint_S \vec{E} \cdot d\vec{A} = \int_0^{2\pi} \int_0^{t_a} E_r \; r \, d\theta \, dz = E_r \; 2\,\pi \, r \, t_a \quad . \tag{A2}$$

where it has been assumed that E_r is constant in both the azimuthal and axial directions. If it is also assumed that the ion charge density is uniform throughout the volume, the right-hand side of Eq. (A1) can also be integrated over this pillbox of radius r to obtain

$$\frac{1}{\varepsilon_o} \int_V \rho \, dV = \frac{1}{\varepsilon_o} \int_V \rho \, r \, dr \, d\theta \, dz = \frac{\rho}{\varepsilon_o} \pi \, r^2 \; t_a \, . \tag{A3}$$

By equating Eqs. (A2) and (A3), one obtains the following expression for the radial electric field strength in the region extending from the accel hole centerline to the outer edge of the beamlet

$$E_r = \frac{\rho \, r}{2 \, \varepsilon_o}, \qquad \left(0 < r < \frac{d_b}{2} \right). \tag{A4}$$

When the integration is carried out over the region from the centerline to the inner edge of the accel hole, the charge density in the region between the beamlet edge and the accel hole barrel is essentially zero. Assuming that the beam current density is uniform, the value of the integral in Eq. (A3) over the region from $r_b \le r \le r_a$ has the form

$$\frac{1}{\varepsilon_o} \int_V \rho \, dV = \frac{1}{\varepsilon_o} \int_V \rho \, r \, dr \, d\theta \, dz = \frac{\rho}{\varepsilon_o} \pi \left[\frac{d_b}{2} \right]^2 \; t_a \, .$$

When this result is equated to (A2), the radial electric field strength is found to be

$$E_r = \frac{\rho\, d_b^2}{8\,\varepsilon_o\, r}, \qquad \left(\frac{d_b}{2} \le r \le \frac{d_a}{2}\right). \tag{A5}$$

The voltage difference from the accel grid barrel to the centerline due to the ion space charge is obtained by integrating the electric field between these limits. Hence

$$\Delta V = -\int_{d_a/2}^{d_b/2} E_r\, dr - \int_{d_b/2}^{0} E_r\, dr = -\int_{d_a/2}^{d_b/2} \frac{\rho\, d_b^2}{8\,\varepsilon_o\, r}\, dr - \int_{d_b/2}^{0} \frac{\rho\, r}{2\,\varepsilon_o}\, dr$$

where the electric fields appropriate to the indicated limits have been substituted using Eqs. (A4) and (A5). Performing the indicated integrations yields

$$\Delta V = \frac{\rho\, d_b^2}{8\,\varepsilon_o}\left[\frac{1}{2} + \ell n\left(\frac{d_a}{d_b}\right)\right] . \tag{A6}$$

The mean charge density that appears in Eq. (A6) is determined by the beamlet ion current (J_b) through the equation

$$\rho = \frac{4\, J_b}{\pi\, d_b^2\, v} .$$

The ion velocity that appears in this equation is given by

$$v = \sqrt{\frac{2\, e\, (V_{dp} - V_{sp})}{m}}$$

where e is the ion charge and m is the mass. Substitution of these equations into (A6) yields the following expression for the barrel-to-centerline potential difference induced by the ion space charge in the accel grid aperture.

$$\Delta V = \frac{J_b}{2\,\pi\,\varepsilon_o}\left[\frac{m}{2\, e\, (V_{dp} - V_{sp})}\right]^{1/2}\left[\frac{1}{2} - \ell n\left(\frac{d_b}{d_a}\right)\right] \tag{A7}$$

It should be noted that the potential difference between the beam axis and edge is purely a function of the amount of enclosed charge. If the detailed beam density profile is known, this function can be inserted into the RHS of Eq. (A1) and integrated in a similar manner as above to derive a more accurate value for the potential difference between the beam axis and edge.